York, 1967), p. 267.
[3]H. H. Woodbury and G. W. Ludwig, Bull. Am. Phys. Soc. 6, 118 (1961).
[4]K. Morigaki, J. Phys. Soc. Japan 19, 2064 (1964).
[5]G. R. Wagner, J. Murphy, and J. G. Castle, Jr., Aerospace Research Laboratories Report No. ARL 70-0108 (unpublished).
[6]W. E. Blumberg, Phys. Rev. 119, 79 (1960).
[7]I. J. Lowe and D. Tse, Phys. Rev. 166, 279 (1968). (See also references therein.)
[8]J. H. Van Vleck, J. Chem. Phys. 7, 72 (1939).
[9]C. B. P. Finn, R. Orbach, and W. P. Wolf, Proc. Phys. Soc. (London) A77, 26 (1961).
[10]Available from National Bureau of Standards, Washington, D. C. , Circular No. 595.
[11]Analysis carried out by Bell & Howell, Electronic Materials Division, 360 Sierra Madre Villa, Pasadena, California 91109.
[12]F. D. Adams, D. C. Look, L. C. Brown, and D. R. Locker, Phys. Rev. B 4, 2115 (1971).
[13]E. Fukushima and A. E. Uehling, Phys. Rev. 173, 366 (1968).
[14]General Electric Co., Chemical Division, Pittsfield, Mass.
[15]The effective lattice constant would actually be somewhat greater than $a = 4.8$ Å because the Cd^{113} isotope is only 12.3% abundant.
[16]D. Gerlich, J. Phys. Chem. Solids 28, 2575 (1967).
[17]Y. K. Shaulov and E. N. Kostina, Russ. J. Phys. Chem. 42, 1077 (1968).
[18]M. M. Kreitman (private communication).
[19]M. A. Nusimovici and J. L. Birman, in *Proceedings of the International Conference on II-VI Semiconducting Compounds*, edited by D. G. Thomas (Benjamin, New York, 1967), p. 1024.

PHYSICAL REVIEW B VOLUME 6, NUMBER 3 1 AUGUST 1972

Channeling in Si Overlaid with Al and Au Films*

E. Rimini, † E. Lugujjo, ‡ and J. W. Mayer
California Institute of Technology, Pasadena, California 91109
(Received 20 December 1971)

Channeling measurements by backscattering of 1.8-MeV He ions have been made on ⟨111⟩- and ⟨110⟩-oriented Si covered with evaporated layers of Al and Au. The minimum yield, half-width of the angular-yield profile, and depth dependence of the aligned yield were measured as a function of metal-film thickness. Comparisons between experimental and calculated values have been made on the basis of two different treatments of plural scattering. The minimum yield follows the predictions of the Meyer treatment. This treatment leads to good agreement with angular-yield profiles and dechanneling dependence on depth obtained with Al films. For Au films the measurements suggest that the distribution should be more peaked than that calculated. These results can also be applied to investigations of dechanneling and disorder in single crystals.

I. INTRODUCTION

Channeling-effect measurements in single crystals are based on the large attenuation in the yield of processes requiring close-impact collisions which are observed when the incident beam is aligned with low-order crystallographic planes or axes; for example, Ref. 1. This attenuation is sensitive to crystalline imperfections and has been used to determine disorder distributions in ion-implanted samples[2-4] and in epitaxially grown single-crystal layers.[5] The yield of close-encounter processes is, in fact, influenced by the initial distribution in transverse momentum of the particles as they enter the crystal. Superposition of amorphous layers on single crystals causes an increase in the particle transverse momentum due to scattering events in the film, in addition to that acquired passing through the crystal surface. This leads to an increase in the aligned yield as has been found for silicon covered with dielectric layers[6,7] and metal films.[8]

Analysis of measurements of disorder distributions and of channeling effects in crystals covered with amorphous layers requires knowledge of the scattered-particle distribution and of the probability that a particle with a given transverse momentum will be transferred out of the aligned component into the random component of the beam (dechanneled). For the dechannneling probability it is assumed (square-well approximation) that a particle is in the random component of the beam when its angle with the channel axis is greater than $\psi_{1/2}$, the critical angle for channeling. In channeling measurements of disorder, various scattering treatments have been used to obtain the angular distributions of the particles; single,[2,9] multiple,[2,3] and plural[4] scattering. These scattering regimes are classified according to the mean value m of the number of collisions, which is proportional to the layer thickness t and to the number of scattering centers per unit volume N. This number m, also

called "reduced thickness," is given by $Nt\pi(a_{TF})^2$, where a_{TF} is the Thomas-Fermi screening parameter. For $m \ll 1$ we are in the region of single scattering which is described for a Coulombic potential by the Rutherford law. For $m \gg 1$ ($m > 20$), the number of scattering events is large and the process is called multiple scattering. In between single- and multiple-scattering regions lies plural scattering.

A plural-scattering regime seems most reasonable to apply to the small numbers of scattering centers typically encountered in disorder analyses. To data, the plural scattering has been based on the treatment of Keil *et al.*,[10] which has a strongly peaked forward distribution. Recently, a new treatment of plural scattering has been proposed by Meyer.[11] Experimental measurements of scattering of heavy ions of keV energies transmitted through thin films show good agreement with calculations based on the Meyer treatment.[12,13] For larger numbers of scattering centers, the two treatments give the same distribution which merges with the Molière theory.[14] For a general reference to multiple scattering in the high-energy regime, see Scott.[15] It seems, then, interesting to study by channeling a more simple experimental situation than that met in disorder analysis. This has been achieved by covering the single crystals with an evaporated layer to simulate the disorder, with the aim to obtain a direct test of the more appropriate distribution to be used to extract disorder profile by channeling-effect measurements.

In this work we have used backscattering techniques with MeV He ions to measure minimum yields, angular-yield profiles, and aligned yields versus depth in silicon samples covered with Au and Al films. The approach was to use various film thicknesses to investigate experimentally the scattering regime where both Meyer and Keil *et al.*, treatments gave comparable distributions and where the distributions differed.

II. EXPERIMENTAL

A. Technique

The samples were prepared by vacuum deposition of different thicknesses of Al and Au layers onto a silicon or germanium single-crystal substrate at room temperature. The evaporation of Al and Au was made on samples masked so that in the same sample there was uncovered Si, Si plus Au, and Si plus Al. The sample was initially aligned along a major axis in the uncovered part and then the incident beam was translated to various portions of the sample to allow a direct comparison of the yields. Film thicknesses ranged between 100 and 1000 Å for Au and between 900 and 5000 Å for Al.

Channeling measurements were made using the backscattering technique with a beam of 1.8-MeV He ions.[1,7] The beam divergence was limited by means of apertures to a value of 0.7×10^{-3} rad. Secondary-electron-suppression techniques were used and the vacuum in the scattering chamber was less than 10^{-5} Torr. Particles backscattered from the target through a laboratory angle of 168° were detected by a 25-mm^2 surface-barrier detector, 10-cm distance, and standard electronics were used to feed pulses to a 400-channel pulse-height analyzer. The energy resolution of the system was $\lesssim 15$ keV.

Figure 1(a) shows two energy spectra of backscattered particles from uncovered Si obtained; (i) when a low-index direction (⟨111⟩) is well aligned with the incident-beam direction (aligned spectrum) and (ii) when the beam is incident in a random direction (random spectrum). The random spectrum was obtained by tilting the sample to 10° and continuously rotating the crystal about the beam direction.[16] Near the surface, the ⟨111⟩ aligned

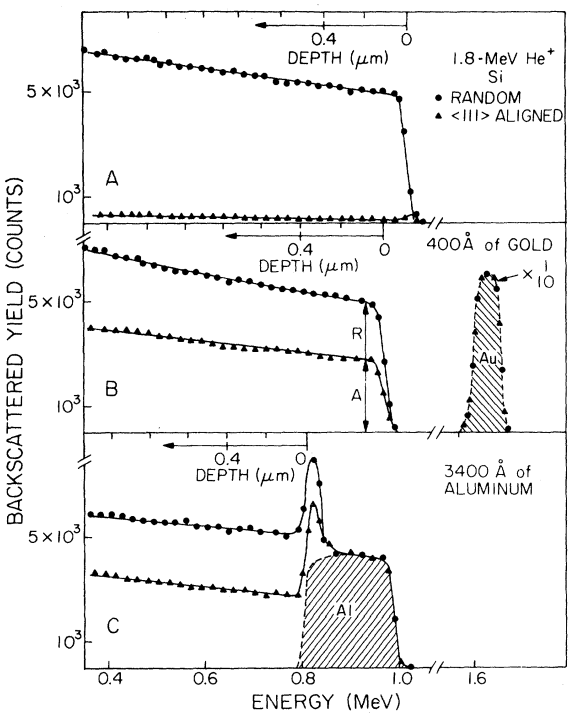

FIG. 1. Energy spectra for 1.8-MeV He$^+$ backscattered; (a) from an uncovered silicon crystal for random (•) and ⟨111⟩ aligned direction (▲), (b) from a silicon crystal covered with 400 Å of Au for random (•) and ⟨111⟩ aligned direction (▲), and (c) from a silicon crystal covered with 3600 Å of Al for random (•) and ⟨111⟩ aligned direction (▲). The bottom scale represents the energy (MeV) of the backscattered particles. The top scale in the three figures represents the depth inside the silicon crystal from which the particle has been scattered.

yield was ~ 3% of the random yield. The ratios of aligned to random yield for ⟨111⟩ and ⟨110⟩ orientations were in agreement with previously measured values.[1]

The energy-to-depth conversion scale is obtained from stopping power[17] and experimental geometry following the usual procedure[18] (representative values for stopping power are 31.4, 29.5, 26.2 eV/Å for 0.5, 1.0, and 1.5-MeV He, respectively). The depth scale for random incidence is shown in Fig. 1(a). For aligned incidence, the depth scale may differ by as much as 15% due to the lower stopping power of well-channeled particles[18] in the ingoing trajectory. However, the stopping power depends on the trajectory of the channeled particle and the exact value to be used in backscattering measurements cannot be specified. We assumed equal aligned and random stopping powers and obtained a depth conversion near the surface of Si of 43.8 eV/Å for both random and aligned spectra.

The angular-yield profiles of uncovered portions were determined by measuring the yield of particles backscattered from just below the surface for fixed integrated beam charge at different tilt angles with respect to the ⟨111⟩ or ⟨110⟩ directions (Fig. 2). The value of full width at half-minimum ($2\psi_{1/2}$) obtained from axial-angular scans agreed with the values obtained in the previous measurements.[1] Values of the aligned yield and $\psi_{1/2}$ on uncovered portions of the samples indicated that the effects of surface-oxide layers, mosaic spread, and lattice disorder were minimal.

The angular scans on the uncovered portion were used to determine sample orientation for aligned and random spectra. These spectra for covered portions of the sample were obtained by translating the beam from the uncovered portion. Translation of the beam causes a change in the angle of incidence of 0.3×10^{-3} rad (a value about 40 times smaller than $\psi_{1/2}$). Measurements on uncovered samples revealed that translation of the beam had no effect on the aligned yield and shape of the angular-yield profile.

To evaluate the evaporated films, backscattering techniques were used.[7,13] Figures 1(b) and 1(c) show spectra of Si samples covered with 400 Å of Au and 3400 Å of Al, respectively. The presence of a metal film causes a shift in the Si signal to lower energy [Fig. 1(b)] due to energy losses of the particles as they transverse the film. The signal from Au [shaded portion, Fig. 1(b)] appears at high energies. The signal for Al [shaded portion, Fig. 1(c)] appears at lower energies and the trailing edge of the Al signal overlaps the leading edge of the Si signal by 21.6 keV producing an overlap peak.[7] The extraction of the aluminum signal from the experimental spectra requires a more elaborate method reported in detail in Ref. 7, and which has been adopted in the present work. The number of Au and Al atoms per cm^2 was determined by integrating the counts in the two signals; this number was used in the comparison with theory, although for simplicity in presentation the film thickness is given in Å (conversion factors: 5.9×10^{17} Au atoms/cm^2 and 6.02×10^{17} Al atoms/cm^2 are equivalent to 1000 Å. Backscattering measurements were also used to determine the uniformity of the film. There were no anomalous features in the trailing edge of Au spectra or in the Al-Si overlap peak for film thicknesses greater than 200 Å of Au and 600 Å of Al, respectively. For Au films of about 100-Å thickness, the leading edge of the Si signal indicates the presence of thickness variations. For this thickness, the spectra for some samples indicated that as much as 10% of the Si was uncovered.

From a channeling standpoint, the films could be treated as amorphous layers. When the beam was aligned with the ⟨110⟩ or ⟨111⟩ axial directions, no change was found in either the Au or Al signals from that obtained with a random incidence. Planar scans also did not reveal orientation effects. These facts indicate that if the films are polycrystalline, the crystallites are either sufficiently small or the orientation is sufficiently random so as to allow

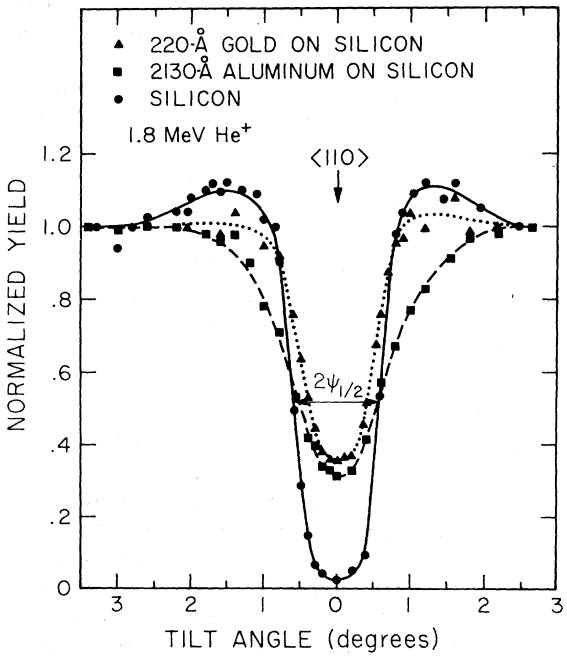

FIG. 2. Normalized yield vs tilt angle for 1.8 MeV He$^+$ impinging on the ⟨110⟩ direction of Si covered with 220 Å of Au (▲) and 2130 Å of Al (■). The yields were measured at depths about 0.1 μ below the surface and normalized to 2500 counts.

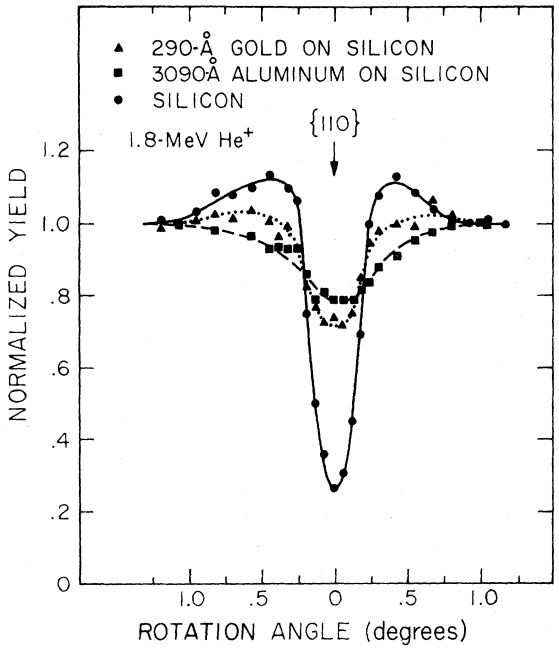

FIG. 3. Normalized yield vs rotation angle for 1.8 MeV He^+ impinging on the {110} plane of Si covered with 290 Å of Au (▲) and 3090 Å of Al (■).

the treatment of these films as amorphous structures.

B. Experimental Concepts

If the crystal is covered by an amorphous layer, the aligned yield [as shown in Figs. 1(b) and 1(c)] increases. This increase is produced by the scattering experienced by a particle traversing the amorphous layer; in fact, the layer introduces an angular dispersion into the initially well-collimated beam so that the fraction of the beam which satisfies the channeling condition is decreased. The measured quantities in channeling experiments are essentially the following: (i) the ratio (minimum yield, or dechanneled fraction χ_0) between the aligned (A) and the random (R) yield near the surface [see Fig. 1(b)]; (ii) the shape of the yield plotted as a function of angle of incidence both for planar and axial direction (see Figs. 2 and 3); (iii) the change in the ratio between aligned (A) and random (R) yields $\chi = A/R$ as a function of depth inside the crystal (see Fig. 4).

Figure 2 shows the normalized yield versus tilt angle for 1.8-MeV He^+ impinging along the ⟨110⟩ direction of a Si sample covered with 220 Å of Au and with 2130 Å of Al. A planar scan across the {110} plane of Si is shown in Fig. 3. The shapes of the planar and of the axial angular-yield profiles differ between uncovered and covered Si not only for the minimum yield, but also for the value of the width, defined as the full width at a level midway between the random and the aligned yield. It is also apparent from the same figures that with nearly the same minimum yield the angular shape is broader for Al case than for Au. The difference in channeling behavior is more evident from Fig. 4 in which the normalized aligned yield (dechanneled fraction) versus depth is plotted for different thicknesses of Al and Au layers on ⟨111⟩ and ⟨110⟩ oriented silicon. The rate of dechanneling is higher for Si covered with aluminum than for Si covered with gold layers. All these observations point out the role played by the amorphous layer in determining the angular distributions of particles.

The results shown in Fig. 4 also indicate that the magnitude of $\psi_{1/2}$ is an important parameter. For instance, the minimum yield measured on Si covered with 340 Å of Au (Fig. 4) is smaller for ⟨110⟩ oriented silicon than for ⟨111⟩ oriented. This is a consequence of the fact that $\psi_{1/2}$ for the ⟨110⟩ orientation is larger than that for ⟨111⟩ orientation. In the following sections we will try to correlate this information with the existing treatments on scattering of particles through thin films.

III. THEORY AND EXPERIMENT

A. General Considerations

The increase in aligned yield for single-crystal substrate covered with amorphous films is de-

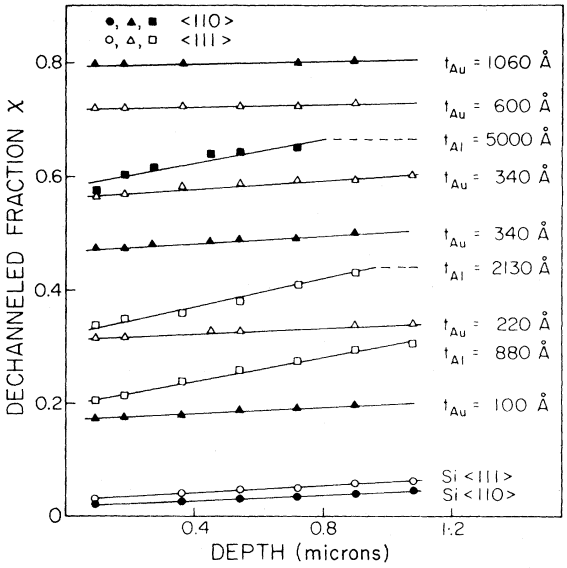

FIG. 4. Ratio of aligned to random yield, the dechanneled fraction vs depth for 1.8 MeV He^+ impinging along the ⟨110⟩ and the ⟨111⟩ axes of uncovered and covered silicon with different thicknesses of Au and Al. (Si: • ⟨110⟩, ○⟨111⟩; Si with Au: ▲ ⟨110⟩, △ ⟨111⟩; Si with Al: ■ ⟨110⟩, □ ⟨111⟩.) The minimum yield at the surface is found by extrapolating the dechanneled-fraction curves to zero depth.

termined by the angular distribution of particles scattered within the film in addition to the deflections produced by the crystal potential and the criterion for channeling within the crystal.

There are several methods to determine the aligned yield from the underlying crystals. One method for calculating the aligned yield near the surface, i.e., the minimum yield χ_0, is to treat as dechanneled all particles just beneath the crystal surface which have an angle with the channel axis greater than $\psi_{1/2}$. The minimum yield is then given directly by the integral of the initial angular differential distribution of particles, just beneath the crystal surface, for angle values greater than $\psi_{1/2}$.

This procedure, usually called the square-well approximation, assumes that a particle is in the random component of the beam (dechanneling probability equal to one) when its angle with the channel axis is greater than $\psi_{1/2}$, or equivalently when its transverse energy $E_\perp$ is greater than $E\psi_{1/2}^2$, and that a particle is in the aligned component (dechanneling probability and rate of interaction equal, respectively, to zero) when its angle with the channel axis is less than $\psi_{1/2}$, or equivalently when the transverse energy $E_\perp$ is less than $E\psi_{1/2}^2$. No account is, then , given for the shape of the dechanneling probability.

The angular distribution of particles which enter a covered single crystal along a close-packed atomic row just beneath the crystal surface results from (i) the experimental angular spread of the beam, (ii) the angular spreading produced by the layer covering the crystal surface, (iii) the scattering due to the lattice potential (transmission factor). In highly perfect crystals not covered with layers, the dechannneling produced by the last mechanism is small [~3% in Fig. 1(a)] for axial channeling, while it amounts to ~20% for planar channeling.

As an approximation for the axial case we have neglected in the covered crystals the contributions (i) and (iii) to the angular distribution of particles, i.e., we have taken into account only the scattering produced by the metal layer in calculating the minimum yield χ_0 (Sec. III B). To test the validity of this approximation a numerical calculation has been carried out including both (ii) and (iii) contributions to determine the angular distribution of particles after traversing 88 Å of Au, and impinging along the ⟨111⟩ axis of Si.[19] The resulting distribution differs about 20% from that obtained with contribution (ii) alone for small angles of scattering ($\sim\frac{1}{10}$ of $\psi_{1/2}$), while the two coincide within 5–10% for angles comparable or greater than $\psi_{1/2}$. Of course with increasing layer thickness the contribution of the transmission factor in the axial case becomes more and more negligible.

In the planar case (treated in Sec. III C), however, the transmission factor cannot be neglected and it is necessary to take the convolution of the angular-planar-yield profile for the uncovered crystal (which includes the transmission factor) with the distribution $f_p(\theta_p)$ of particles scattered through an angle θ_p with respect to the plane.

The same convolution treatment can be applied to the axial case (Sec. III D) to obtain the minimum yield at the surface. Further, the treatment can be extended to give the aligned yield as a function of depth within the crystal (the depth dependence of dechanneling). In this case the angular-yield profile measured on an uncovered crystal at various depths within the crystal is utilized as the probability for dechanneling in which all the contributions previously neglected are taken into account.

The differential angular distributions obtained directly from the Meyer and the Keil *et al.* treatment of plural scattering are shown in Fig. 5. In these treatments film thicknesses are specified by the parameter m which is proportional to the number of scattering centers through the relation m

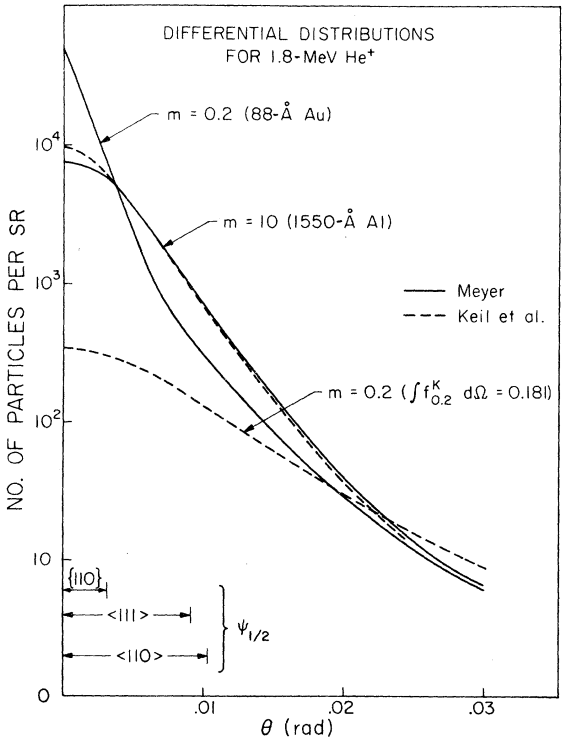

FIG. 5. Differential angular distribution $f(\theta)$ for 1.8 MeV He^+ ions after traversing a reduced thickness $m=0.2$ (88 Å of Au) and $m=10$ (1550 Å of Al) according to the Meyer (Ref. 11) treatment (full lines) and the Keil *et al.* (Ref. 10) treatment (dashed lines). The integral of the differential distribution for $m=0.2$ is 0.181 in the Keil *et al.* treatment. The experimental values of the critical angle for Si ⟨111⟩, ⟨110⟩, and {110} are shown on the bottom left.

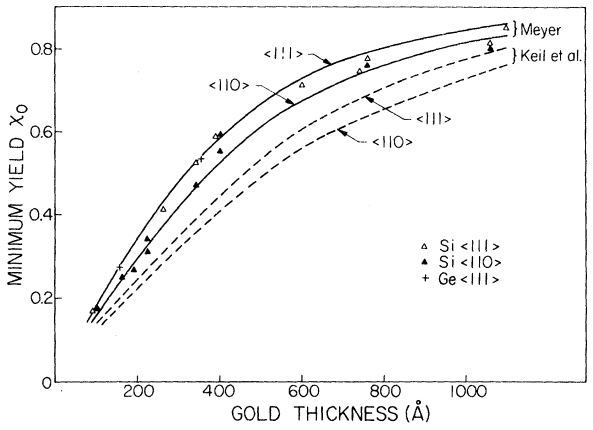

FIG. 6. Minimum yield χ_0 at the silicon surface for 1.8 MeV He^+ impinging along the ⟨110⟩ (▲) and ⟨111⟩ (Δ) axes of Si covered with different thicknesses of Au. The lines show the calculated values using the square-well approximation, and the Meyer distribution (solid line), and the Keil *et al.* distribution (dashed line). The square-well approximation assumes that particles scattered beyond $\psi_{1/2}$ are dechanneled.

$= \pi N a_{TF}^2 t$, where a_{TF} is the Thomas-Fermi screening parameter ($a_{TF} = 0.105$ Å for Au and $a_{TF} = 0.176$ Å for Al), N is the number of atoms per $(Å)^{-3}$, and t is the film thickness in angstroms. Physically, m is the mean value of the number of collisions of the particles with the target atoms for a cross section of $\pi(a_{TF})^2$.

The two treatments differ in the choice of the scattering cross section. Keil *et al.* used the Molière cross section which is smaller than the Thomas-Fermi[20] cross section used by Meyer. As a result, for low values of m the Keil treatment predicts that a large fraction (proportional to e^{-m}) of the beam passes through the film without deflection. In Fig. 5 for $m = 0.2$ the integrated distribution $\int_0^\infty f_{0.2}^K(\theta) 2\pi\theta\, d\theta$ is 0.18, indicating that 82% of the particles are undeflected for an 88-Å thick Au film. On the other hand, in the Meyer treatment, all the particles are scattered ($\int_0^\infty f_{0.2}^M(\theta) 2\pi\theta\, d\theta = 1$). In both cases, the distribution becomes broader with increasing values of m. For large values of m ($m > 20$, Au $\simeq$ 9000 Å, and Al $\simeq$ 3500 Å), the two distributions approach the Molière analytical computations.

The differential distributions of the particles in the film can be represented as a function of the reduced scattering angle, because the form of the scattering distribution is then independent of energy.[10–13] However, it is important to note that the reduced scattering angle is a function of energy as well as the atomic number of the scattering film. For instance, the reduced scattering angle for Al is ten times larger than that for Au for 1.8-MeV He^+. Figure 5 shows the scattering distribution in terms of laboratory angles for comparison with values of channeling half-angles ($\psi_{1/2}$).

B. Axial-Minimum Yield, Square-Well Approximation

In the square-well approximation the measured dechanneled fraction χ_0 at the surface of the silicon crystal is determined, neglecting the transmission factor, by the number of particles incident with an angle greater than the critical angle $\psi_{1/2}$. Figure 6 shows values of the minimum yield for ⟨111⟩ and ⟨110⟩ orientation versus thickness of the Au film calculated by integrating the differential distribution out from $\psi_{1/2}$. The solid lines represent the values calculated from Meyer and the dashed lines are the values from Keil *et al.* In these calculations we have used experimental values[1] of $\psi_{1/2}$ for particle energies after traversing the film. (In Fig. 5 the values of $\psi_{1/2}$ for 1.8 MeV are shown for ⟨111⟩, ⟨110⟩, and {110} directions.) The experimental points follow the trend of both theories but agree in absolute magnitude more closely with the Meyer treatment. Two points (+) for Ge ⟨111⟩ are included, since $\psi_{1/2}$ for this case lies between the Si ⟨110⟩ and ⟨111⟩ values. These points also are closer to the Meyer theory.

For aluminum the experimental and calculated values of χ_0 versus thickness are shown in Fig. 7. In this case the difference in the two calculations is not great. In fact the difference in the calculated values of the minimum yield between ⟨110⟩ and ⟨111⟩ orientations is much greater than the difference between minimum yield values predicted by the two treatments. The measured values agree with 10% with theory for both crystal orientations for film thicknesses greater than 1000 Å. The experimental points for Au and Al are not corrected

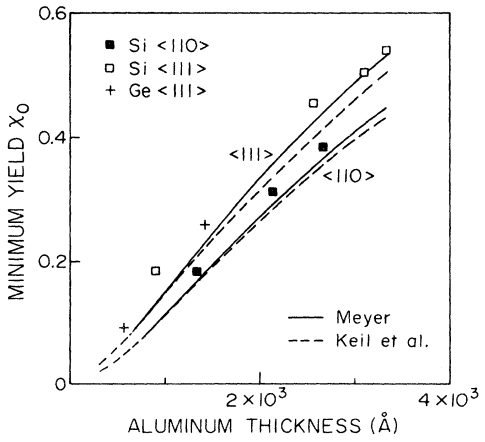

FIG. 7. Minimum yield χ_0 for 1.8 MeV He^+ impinging along the ⟨110⟩ (■) and ⟨111⟩ (□) axes of Si crystals covered with different thicknesses of Al. The solid lines represent the values calculated from Meyer and the dashed lines, the values from Keil *et al.*

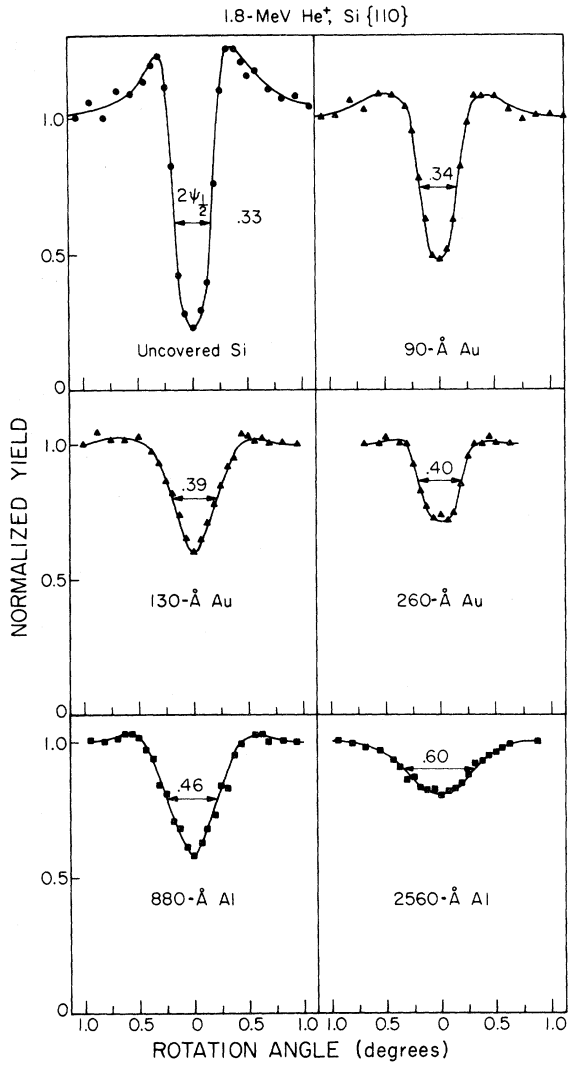

FIG. 8. {110} planar-angular-normalized-yield profiles for 1.8 MeV He^+ on uncovered and covered silicon crystals with different thicknesses of Au and Al layers. The minimum yield, and the full-width increase with increasing thicknesses. The yields were measured at depths about 0.1 μm below the surface and normalized to 2500 counts.

for the minimum yield (2–3.5%) from uncovered Si, i.e., the correction for the surface transmission factor. For Al this correction would bring the experimental points closer to the calculated curve especially in the region of low thickness.

For the planar case, the minimum yield for uncovered Si is relatively large due to the surface transmission factor.[21] Even for the most favorable case, the {110}, the planar minimum yield is $\simeq 0.22$ for 1.8 MeV He ions. In this case then, the minimum yield can be calculated from the convolution of the projected planar scattering distribution and the planar-angular-yield profile for uncovered Si. This is treated more fully in Sec. III C.

C. Planar-Angular-Yield Profile

Another method of investigating the influence of amorphous layers is provided by measurements of the yield at the Si surface as a function of orientation between beam and crystal target. Such curves of the angular-yield profile are shown for one thickness of Au and Al in Fig. 2 (axial scan across the ⟨110⟩) and Fig. 3 (planar scan across the {110}). The angular yield profile is broader for covered Si than for uncovered Si. Further, the full width of the angular profile is greater for Si covered with Al than for Si covered with Au, although they have nearly the same χ_0.

We have investigated the planar case experimentally in more detail, because the comparison with theory requires calculations which are more straightforward than those required in the axial case. Figure 8 shows a series of {110} planar profiles in Si, both uncovered and covered with different thicknesses of Au and Al layers. The minimum planar yield increases with increasing film thicknesses, the shoulders disappear and the full width increases. To compare these experimental angular-yield profiles with calculations, it is necessary to determine the number of particles scattered through the angle θ_p with respect to the plane, i.e., the projection of the angle θ on a surface both normal to the plane and parallel to the beam direction,

$$f_p(\theta_p) = 2\int_0^\infty d\phi f[(\theta_p^2 + \phi^2)^{1/2}] \quad .$$

The projected planar distributions for 1.8 MeV He^+ traversing a reduced thickness $m = 0.6$ (264 Å of Au) are shown in Fig. 9 for Meyer and Keil *et al.* treatments. For $m = 0.6$ we have $2\int_0^\infty f_p^M(\theta_p)d\theta_p = 1$ and $2\int_0^\infty f_p^K(\theta_p)d\theta_p = 0.45$. The arrow in the Keil *et al* distribution indicates the undeflected part of the beam which amounts to 55%. An experimental planar-angular-yield profile, measured for 1.8 MeV He^+ on uncovered Si is shown in the lower part of Fig. 9. This profile is used as the probability that a particle inclined at an angle θ_p to the plane is dechanneled.

Figure 10 shows the calculated and experimental planar-angular profiles for 1.8 MeV He^+ in Si ⟨110⟩ covered with Au (260 Å) and with Al (2560 Å). The minimum-yield value is obtained by convolution of the projected planar distribution with the experimental planar scan for uncovered Si. The yield for any angle θ' of incidence is also obtained by the convolution of the probability curve with the projected-planar-distribution function displayed by an amount θ'. For the aluminum case both calculated curves closely coincide and are in satisfactory agreement with the experimental one. The calculated angular-yield profile for the Keil *et al.* treatment applied to the Au case gives a smaller mini-

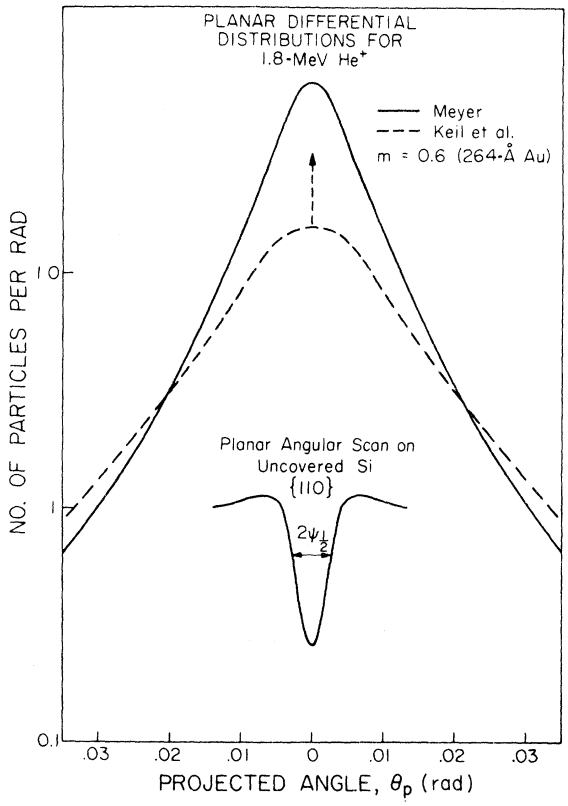

FIG. 9. Planar differential distributions $f_p(\theta_p)$ for 1.8 MeV He^+ ions after traversing a reduced thickness $m = 0.6$ equivalent to 264 Å of Au, according to Meyer (full line) and Keil *et al.* (dashed line) treatment. The dashed arrow in the Keil *et al.* curve represents the undeflected part of the beam. A planar-angular scan on uncovered Si is shown in the lower part of the figure. This profile is used as the probability that a particle inclined at an angle θ_p to the plane is dechanneled.

mum yield and a narrower half-width than that for the Meyer treatment. The experimental value of the planar minimum yield agrees closely with that predicted from the Meyer treatment. This agreement might be expected on the basis of axial minimum yield values discussed previously. However, the experimental width of the planar angular yield is narrower than that calculated. This suggests that the scattering distribution is more peaked than that of the Meyer treatment.

D. Dechanneling

The calculated, axial, minimum-yield values gave information on the number of particles scattered beyond $\psi_{1/2}$ and the calculated planar-angular-yield profile utilized the entire scattering distribution. Another method of investigating the scattering distribution for angles less than $\psi_{1/2}$ is provided by the increase in minimum yield as a function of depth. In our case the dechanneling dependence on depth can be calculated in two different ways: (a) utilization of dechanneling calculations based on the increase of transverse energy with depth and (b) utilization of experimental profiles as a function of depth.

1. Transverse Energy

The scattering angle θ of a particle traversing a film is related to its initial transverse energy $E_\perp$ inside the crystal, neglecting the deflection produced by the atomic row potential, by the relation $E_\perp = E\theta^2$, where E is the particle energy.

The transverse energy of a channeled particle is not conserved along its path inside the channel and it increases because of the scattering experienced with the vibrating nuclei and electrons of the crystal. Transitions of particles from the aligned to the random component of the beam are then possible as soon as the transverse energy reaches a critical value and as a consequence an increase in the measured aligned yield with depth is observed. Foti *et al.*[19] have calculated the depth at which a particle of given initial transverse energy reaches the critical value $E\psi_1^2/2$ to be dechanneled. The knowledge of the initial transverse-energy distribution allows calculation of the dechanneled fraction as a function of depth. Figure 11 shows the method of determining this fraction. The upper curve is the integral distribution [the number $F(\theta)$ of particles scattered through an angle greater than θ, $F(\theta) = \int_\theta^\infty 2f(\theta)\theta\, d\theta$, where $F(\psi_{1/2}) = \chi_0$], obtained from Meyer for $m = 0.6$ (264 Å of Au). The lower curve (obtained from Grasso *et al.*[22]) gives the depth at which a particle is dechanneled as a function of angle with the channel axis for the ⟨111⟩ direction

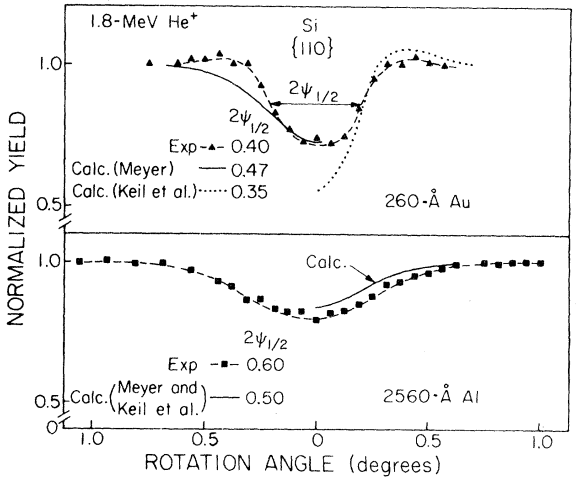

FIG. 10. Experimental and calculated normalized yield vs rotational angle for 1.8 MeV He^+ impinging along the {110} plane of Si crystals covered with 260 Å of Au and 2560 Å of Al.

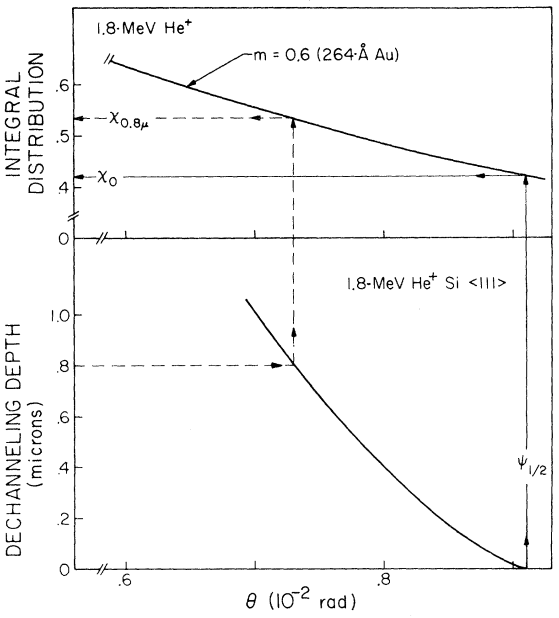

FIG. 11. Integral distribution (upper) using the Meyer treatment vs scattering angle for 1.8 MeV He^+ after traversing a reduced thickness $m = 0.6$ (264 Å of Au). The depth at which (lower) a particle with an incident angle θ to the $\langle 111 \rangle$ reaches the critical angle $\psi_{1/2}$ for dechanneling. These curves are used to determine the yield at any depth.

in Si at room temperature. For instance, to determine the yield at a depth of 0.8 μ, one finds the initial angle (dashed line, lower curve) and then reads up to the integral distribution curve to find the dechanneled fraction, in this case $\chi = 0.54$. The yield χ_0 at the surface is given by reading up from $\psi_{1/2}$ to the intersection with the integral distribution curve.

Similar procedures have been applied to obtain the calculated-dechanneled fractions shown in Fig. 12. The agreement in magnitude between the experimental and the calculated-dechanneled fraction (minimum yield) near the surface has been discussed in Sec. III A. In terms of depth dependence of dechanneling, the shape of the curves for Al agrees well with experimental data. For the 3090-Å-Al film, the absolute values agree. For the 800-Å thick Al film the difference between experimental and calculated values is in part due to the fact that these curves are not corrected for the minimum yield from uncovered Si (neglect of the transmission factor). For the Au case the calculated shapes show a greater dechanneling rate than that of experimental points.

2. *Angular Profile*

The second approach utilizes both the experimental angular-yield profiles obtained at different depth inside the crystal and the calculated differential scattering distribution $2\pi\theta f(\theta)$. In this method the dechanneled fraction at a given depth is obtained by convolution of the initial scattering distribution with the experimental probability that a particle entering with an angle θ is dechanneled at the specified depth. These probability curves have been obtained from experimental energy spectra recorded for different incident angles. In the upper part of Fig. 13 some of these energy spectra are shown for 1.8 MeV He^+ incident at different angles to the $\langle 110 \rangle$ direction in uncovered Si. In the lower part, the normalized yield is plotted as a function of incident angle at three different depths in the crystal.

The differential distributions $2\pi\theta f(\theta)$ plotted in Fig. 14 give the number of particles scattered by the metal layer at an angle θ from the initial direction, independent of the azimuthal angle. These distributions have been taken from Meyer for $m = 0.8$ (352 Å of Au) and $m = 14$ (2160 Å of Al). In the lower part of Fig. 14 the experimental axial probability curve at 0.1 μm inside the crystal, is plotted as a function of the incident angle. Also shown for comparison is the square-well probability (dashed line) used previously in Sec. III B) to compute the minimum yield near the crystal surface. The dechanneled fractions calculated with

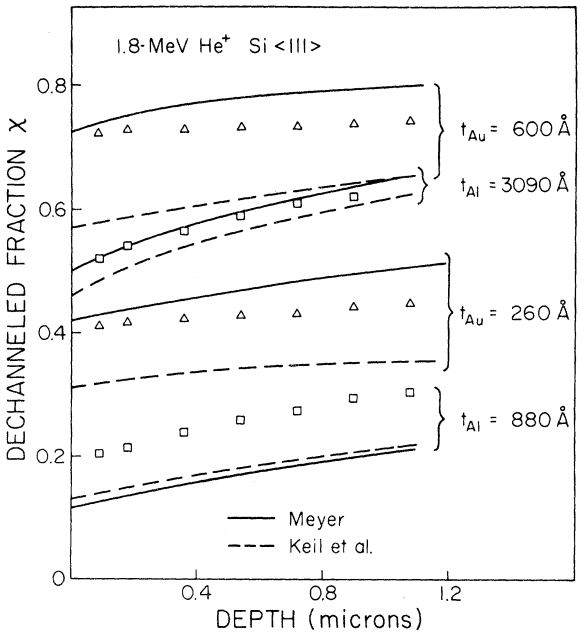

FIG. 12. Experimental and calculated-dechanneled fraction χ vs depth for 1.8 MeV He^+ impinging along the $\langle 111 \rangle$ direction of Si covered with (a) 260 Å and 600 Å of Au (Δ); (b) 880 Å and 3090 Å of Al (□). The full and dashed lines represent the dechanneled fraction calculated according to Meyer and Keil *et al.* treatments, respectively.

this procedure are shown in Fig. 15 for 190 and 360 Å of Au and 2130 Å of Al. The experimental and the calculated data agree quite well for both absolute magnitude and rate of dechanneling in the Al case, while the same difference previously found in the Au case (see Fig. 12) is maintained also in this calculation. This again points out that the scattering distribution for low m values is somewhat more peaked than that predicted by Meyer. This second method is a more accurate procedure for determining the minimum yield in that the actual dechanneling probability is used instead of the square-well approximation and the transmission factor is also taken into account. However, comparison of the minimum yield shown in Fig. 6 and 7 with those found in Fig. 15 indicates that the square-well approximation is adequate for determining the axial minimum yield in cases where the scattering distribution extends well beyond the critical angle.

IV. SUMMARY AND CONCLUSIONS

Channeling measurements in Si single crystals overlaid by thin metal layers indicate that the minimum yield χ_0, the width of the angular-yield

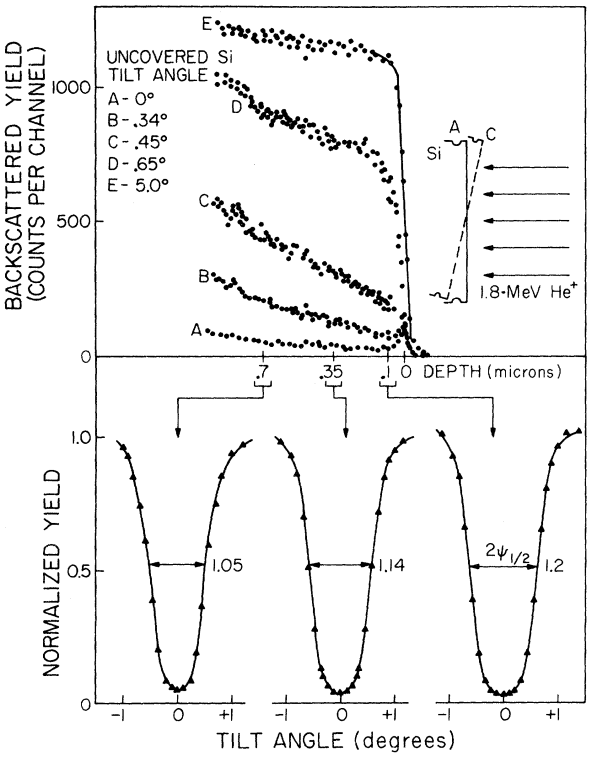

FIG. 13. Energy spectra (upper) for 1.8 MeV He^+ backscattered from an uncovered silicon crystal tilted at various angles with respect to the aligned direction. Normalized yield vs tilt angle (lower) obtained at three different depths for 1.8 MeV He^+ incident on uncovered Si.

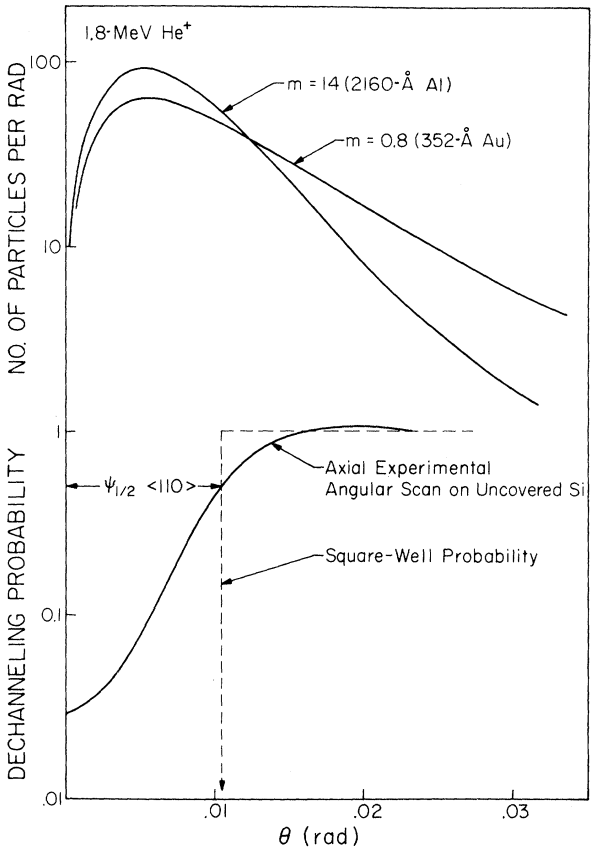

FIG. 14. Number of particles (upper) scattered at an angle θ from initial direction for 1.8 MeV He^+ after traversing a reduced thickness $m = 0.8$ (352 Å of Au) and $m = 14$ (2160 Å of Al) according to Meyer. Experimental axial yield vs incident angle (solid line (lower). This yield profile is used as the probability that a particle incident at an angle θ is dechanneled. The square-well probability is shown as a dashed line.

profile, and the dechanneling dependence on depth are increased over those found in an uncovered crystal. From a qualitative standpoint, these can be understood on the basis of scattering events within the metal film which cause an increase in beam divergence. On a quantitative basis this can be predicted from the scattering distribution of particles and the experimental knowledge of channeling behavior in uncovered silicon.

Using these concepts the plural-scattering regime has been investigated using MeV He^+ ions incident on Si covered with Al and Au layers. In the regions near the surface of Si the axial minimum yield agrees within 10% with calculations based on the Meyer treatment. The angular-yield profiles and dechanneling dependence on depth show similar agreement for thick films but for thinner films the data suggest that the scattering distribution is somehow more peaked than that predicted by Meyer.

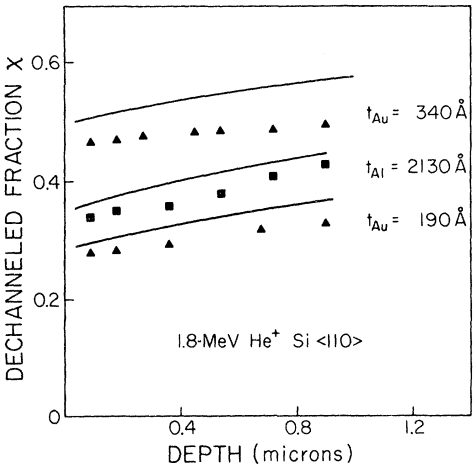

FIG. 15. Dechanneled fraction χ vs penetration depth for 1.8 MeV He^+ impinging along the $\langle 110 \rangle$ of Si covered with different thicknesses of Au (▲) and Al (■) layers. The full lines represent the calculated values of dechanneled fraction χ according to the method of using angular profiles (see text).

The assumption that the minimum yield is determined by the number of particles scattered beyond the critical angle (square-well approximation) has been tested with axial-angular scans. The results indicate that this square-well approximation leads to a reasonable accurate determination of the minimum yield at the surface. For the planar case, surface transmission effects do not allow use of a simple square-well approximation where only the angular distribution produced by scattering in the metal layer is used. In this latter case convolution techniques must be applied.

In this work the increase in the axial aligned yield was analyzed to a depth of about 1 μm. To probe greater depths, a MeV proton could be used. The technique of measuring the yield as a function of depth for different angles of incidence can also be applied to investigate dechanneling processes. For example, measurements of angular profiles as a function of depth, shown in Fig. 13, provides a method of testing the dechanneling-depth calculation shown in the lower part of Fig. 11.

ACKNOWLEDGMENTS

The authors wish to thank F. Grasso and G. Foti for providing calculations of the increase in transverse energy with depth. Discussions with M. -A. Nicolet were greatly appreciated.

---

*Supported in part by the Office of Naval Research Grant No. N00014-69-A-0094-0022 and National Science Foundation Grant No. GP-19887.

†Permanent address: Institute of Physics, University of Catania, Italy.

‡Supported by African-American Institute Fellowship.

[1]S. T. Picraux, J. A. Davies, L. Eriksson, N. G. E. Johansson, and J. W. Mayer, Phys. Rev. 180, 873 (1969).

[2]E. Bøgh, Can. J. Phys. 46, 653 (1968).

[3]L. C. Feldman and J. W. Rodgers, J. Appl. Phys. 41, 3776 (1970).

[4]J. E. Westmoreland, J. W. Mayer, F. H. Eisen, and B. Welch, Rad. Effects 6, 161 (1970).

[5]S. T. Picraux, Appl. Phys. Letters 20, 91 (1972).

[6]O. Meyer, J. Gyulai, and J. W. Mayer, Surface Sci. 22, 263 (1970).

[7]I. V. Mitchell, M. Kamoshida, and J. W. Mayer, J. Appl. Phys. 42, 4378 (1971).

[8]E. Rimini, E. Lugujjo, and J. W. Mayer, Phys. Letters 37A, 152 (1971).

[9]R. Hart, Rad. Effects 6, 51 (1970).

[10]E. Keil, E. Zeitler, and W. Zinn, Z. Naturforsch. 15a, 1031 (1960).

[11]L. Meyer, Phys. Status Solidi B44, 253 (1971).

[12]F. Bernhard, J. Lippold, L. Meyer, S. Schwalse, and R. Stolk, in *Atomic Collision Phenomena in Solids* edited by D. W. Palmer, M. W. Thompson, and P. D. Townsend (North-Holland, Amsterdam, 1970), p. 633.

[13]H. H. Andersen and J. Bøttiger, Phys. Rev. B 4, 2105 (1971).

[14]G. Molière, Z. Naturforsch. 3a, 78 (1968).

[15]W. T. Scott, Rev. Mod. Phys. 35, 231 (1963).

[16]J. Ziegler and B. L. Crowder, Appl. Phys. Letters 20, 178 (1972).

[17]C. F. Williamson, J. P. Boujot, and J. Picard, Centre d'Etudes Nucleaires, Saclay, Report No. CEA-R-304201966 (unpublished) cited by D. A. Thompson and W. D. Mackintosh, in J. Appl. Phys. 42, 3969 (1971).

[18]J. A. Davies, J. Denhartog, and J. L. Whitton, Phys. Rev. 165, 345 (1968).

[19]The method used in this calculation is described in detail by G. Foti, F. Grasso, R. Quattrocchi, and E. Rimini [Phys. Rev. B 3, 2169 (1971)].

[20]J. Lindhard, V. Nielsen, and M. Scharff, Natl. Kgl. Danske Videnskab. Selskab, Mat.-Fys. Medd. 38, No. 10 (1968).

[21]S. T. Picraux and J. U. Andersen, Phys. Rev. 186, 267 (1969).

[22]F. Grasso, G. Foti, and E. Rimini (unpublished).